# ADDRESSING SUMMER COMFORT IN LOW-ENERGY HOUSINGS USING THE AIR VECTOR: A NUMERICAL AND EXPERIMENTAL STUDY

Axel Cablé*, Ghislain Michaux, and Christian Inard

*LaSIE, University of La Rochelle*
*Pôle Sciences et Technologie*
*17042 La Rochelle Cedex 1 - France*

**Corresponding author: axel.cable@gmail.com*

## ABSTRACT

This article deals with summer comfort and room air distribution in low-energy housings. In such buildings, the efficient thermal insulation and air tightness make it crucial to efficiently dispose of the heat released by the internal gains. In this prospect, the comfort in a test room resulting from an integrated cooling and ventilation system is assessed both experimentally and numerically. The air is supplied into the room close to the ceiling through a wall-mounted diffuser of complex geometry composed of 12 lobed nozzles. Experimentally, the air velocity, $CO_2$ concentration, indoor air, wall and globe temperatures are monitored to assess the indoor environment quality. Numerically, CFD software Star-CCM+ is used to provide valuable information on the airflow patterns in the room. The CFD simulations are run in two steps in order to correctly integrate the complex diffuser's geometry. An excellent indoor environment is obtained in the studied conditions. Furthermore, a parametric study is performed in order to investigate the influence of the heat sources and of the supplying conditions on the airflow and on the resulting comfort.

## KEYWORDS

HVAC, air diffusion, summer comfort, experimentations, CFD

## INTRODUCTION

Poor indoor air quality and thermal comfort have an important impact on health, well-being and productivity [1]. It is therefore necessary to supply fresh air to the building and dispose of heat, particles, humidity and other pollutants generated in the building. This issue is particularly crucial for low-energy buildings. In fact, they benefit from good thermal insulation and air tightness. Consequently, the heat released by internal gains (*i.e.* the occupants and electronic devices) cannot easily be disposed of. While this reduces to a great extent the energy required for heating in winter conditions, it also makes it particularly difficult to maintain an acceptable indoor temperature in summer conditions. Therefore, the air distribution system should be able to efficiently evacuate the warm, old air, and ensure a homogeneous cooling of the occupied zone. In this prospect, an integrated cooling and ventilation system is considered, with conditioned air blown through a wall-mounted mixing diffuser. The resulting summer comfort in a room is assessed both experimentally and numerically. The experimental method aims at assessing the thermal comfort and ventilation

efficiency by measuring the flow parameters in the occupied zone of a test room. At the same time, it provides realistic boundary conditions for the CFD simulations, whose purpose is to give additional information on the airflow patterns inside the room and in the jet region. Additional CFD simulations are then performed for supplying conditions which are not tested experimentally, in order to pinpoint the influence of the supplying conditions on the airflow pattern.

## EXPERIMENTAL METHOD

### Test room

The experiments are conducted in an airtight test room composed of steel wall panels (see Fig.1a). An air treatment unit is used to blow the inlet air at the specified temperature and flow rate and the wall temperatures are controlled with a thermal guard enclosing the test room. In order to enhance the mixing of the fresh, cold air, with the indoor air, a wall-mounted diffuser is used. It is composed of 12 complex lobed nozzles with a nozzle to nozzle spacing of 8 cm (see Fig.1b) and the first nozzle is located 16 cm below the ceiling. Two black cylindrical manikins of height 1.1 m and diameter 0.5 m are located inside the room to account for occupancy, with a $CO_2$ emission rate of 18 L/h. Lamps are placed inside the manikins to account for the sensible heat source, corresponding to a metabolism of 1 met.

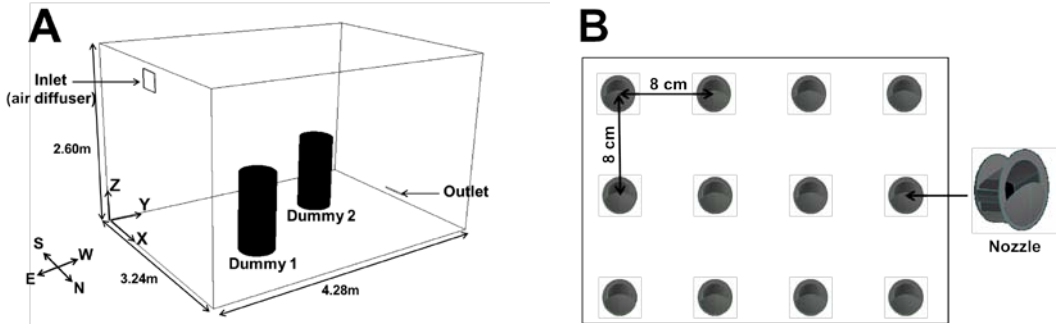


Figure 1. a) Room geometry, b) Diffuser geometry and detail of one nozzle.

### Measurements

Measured variables include boundary conditions measurements at the air inlet, outlet and walls, as well as indoor variables measurements in order to assess the comfort. Air and globe temperature, air velocity and $CO_2$ concentration are monitored on 27 positions inside the occupied zone (Fig.2), corresponding to the ankle level (0.1 m), the neck level of a seated person (1.1 m) and the neck level of a standing person (1.7 m). The results are obtained when steady-state conditions are reached for all the measured values.

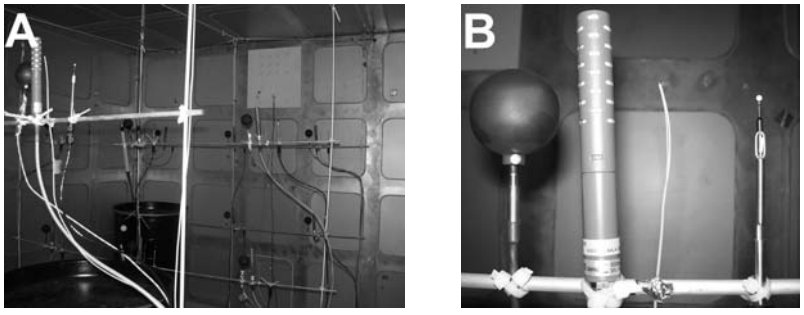


Figure 2. Experimental setup. a) Test room, b) Monitoring position in the occupied zone (globe thermometer, $CO_2$ probe, type-K thermocouple a nd omnidirectional thermal anemometer)

## NUMERICAL METHOD

### Numerical parameters

CFD code STAR-CCM+ is used to solve the 3D transport equations for mass, momentum, energy and $CO_2$ over the computational grid under steady-state conditions. The realizable k-ε turbulence model is chosen, which has been giving good results in room airflow simulations [2]. Two-layer wall functions are employed to model the heat transfer at the walls and buoyancy forces are taken into account through the variation of the density of the fluid considered as an ideal gas. Convergence is ensured by monitoring the residuals and the air and carbon dioxide mass balance evolution.

### Diffuser modelling

The air diffuser is responsible for most heat and mass transfers inside the room, it is therefore crucial to correctly implement its geometry in the CFD simulation. However, the complex details of the diffuser make it too costly to directly include its complete geometry in the simulation. Several diffuser modeling methods have been developed to specify simplified boundary conditions either at the level of the diffuser (Momentum method) or on a surface from a distance of the diffuser (Box Method). However, these methods require either precise measurements at the exit of the diffuser or characteristic equations associated with the diffuser geometry [3]. Since this information is not available, another approach is followed. A first simulation of only one nozzle of the diffuser is performed in a reduced computational domain (3M polyhedral cells), whose outlet boundaries are located 20 equivalent diameters away from the nozzle. The velocity components, turbulence quantities and temperature profiles are then collected at the very exit of the nozzle (Fig.3). Prior simulations have been run with several adjacent nozzles in order to ensure that the flow is not affected by the other nozzles at such a close distance. The collected profiles are then set as inlet boundary conditions in the full room simulation for each of the 12 nozzles (Fig.3c). A similar approach had been successfully used by Cehlin and Mosfegh[4] with a perforated displacement diffuser.

The test room calculation domain is then composed of 3M polyhedral cells (Fig.3c), the grid being refined in regions of high gradients (at the exit of the diffuser, close to the walls and to the dummies). The inlet boundary conditions correspond to the collected profiles, and an atmospheric pressure condition is specified at the exhaust. The other boundary conditions used for the CFD simulations were provided by the experiments.

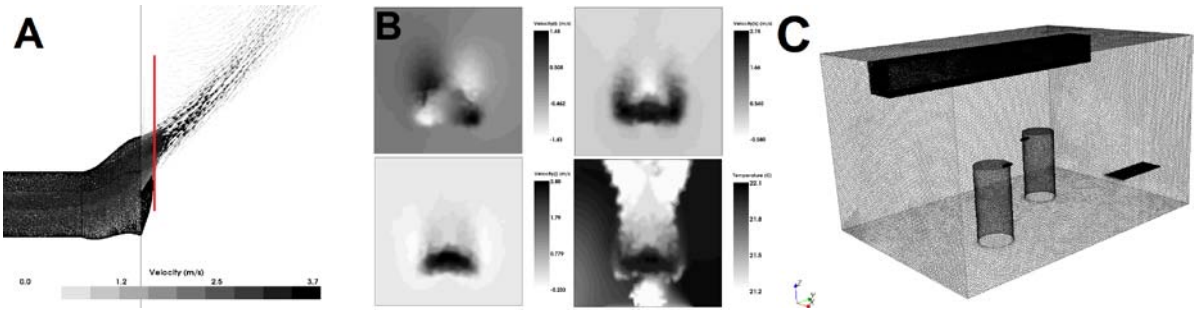


Figure 3. Diffuser modelling approach. a) Single nozzle simulation and profile collecting section, b) Collected velocity components and temperature profiles set as boundary conditions in the full room simulation c) Full room simulation (3M polyhedral cells).

## RESULTS AND DISCUSSION

The obtained results are presented below, and analysed in terms of thermal comfort and ventilation efficiency. The airflow patterns are then investigated with the help of the CFD simulations in order to pinpoint the influence of the internal gains and supplying conditions on the airflow. The conditions of the studied cases are provided in Tab. 2, where $T_{walls}$ corresponds to the average surface temperature of the six walls, and $P_{inlet}$ is calculated as follows :

$$P_{inlet} = Q_0 c_p (T_0 - T_{OZ}) \quad (1)$$

Where $Q_0$ is the inlet air mass flow rate, $T_0$ the inlet temperature, and $T_{OZ}$ the average temperature in the occupied zone. The air flow rate is the same for all cases (1,6 air change per hour), and is chosen in order to provide the cooling power while maintaining the supplied air temperature high enough. The Reynolds number (Eq.3), which qualifies the nature of the flow, and the Archimedes number (Eq.4), which is the ratio of the buoyancy force to the inertia force, are based on the equivalent diameter $D_e$ of the free area of the 12 nozzles $A_{diffuser}$ composing the diffuser (Eq.2).

$$D_e = 2\sqrt{\frac{A_{diffuser}}{\pi}} \quad (2) \; ; \quad Re_0 = \frac{\rho U_0 D_e}{\mu} \quad (3) \; ; \quad Ar_0 = \frac{g\beta_T |T_0 - T_{OZ}| \, 2\sqrt{A_{diffuser}/\pi}}{{U_0}^2} \quad (4)$$

Where $U_0$ is the inlet velocity.

| | $Q_0$ | | | $T_0$ | $T_{exhaust}$ | $T_{guard}$ | $T_{walls}$ | $P_{dummy}$ | $P_0$ | $Q_{CO2}$ | $T_0$ - $T_{oz}$ | $Ar_0$ | $Re_0$ |
|---|---|---|---|---|---|---|---|---|---|---|---|---|---|
| | $m^3/h$ | kg/h | ACH | °C | °C | °C | °C | W | W | l/h | °C | - | - |
| **Case 0** | 55.6 | 66.7 | 1.62 | 21.5 | 24.9 | 28.0 | 25.7 | - | 69 | - | -3.7 | 9.6E-04 | 16384 |
| **Case 1** | 57.0 | 69.4 | 1.66 | 17.0 | 25.3 | 28.0 | 25.9 | 107 | 162 | 18.0 | -8.3 | 2.1E-03 | 17247 |
| **Case 2** | 56.6 | 69.4 | 1.65 | 14.9 | 24.8 | 27.2 | 25.4 | 213 | 200 | 36.0 | -10.3 | 2.7E-03 | 17356 |

Table 1. Boundary conditions for the studied cases

### Global comfort

The EN 15251 standard [5] was used to evaluate the indoor environment quality (IEQ). It provides a classification of the IEQ depending on the values of the operative temperature, Predicted Mean Vote as defined by Fanger [6], and carbon dioxide concentration level. Category I corresponds to an IEQ level expected in schools or buildings with sensitive persons. Category II is the level expected for new or refurbished buildings, while Category III is the value expected for existing buildings. In addition, the ISO 7730 standard [7] defines the Draught Rate as the percentage of dissatisfied for a given air velocity, air temperature and turbulence intensity.

| Category | Maximum operative temperature (cooling season) (°C) | PMV | Maximum $CO_2$ level above outside concentration (ppm) |
|---|---|---|---|
| I | 25.5 | < 0.2 | 300 |
| II | 26 | < 0.5 | 500 |
| III | 27 | < 0.7 | 800 |

Table 2. IEQ categories according to the EN 15251 standard[5]

The contaminant removal effectivness (Eq.5) and temperature efficiency (Eq.6) as defined by Sandberg [8] are also considered, and express the ability of the air distribution system to dispose of a pollutant, and to cool the indoor air, respectively :

$$\varepsilon_C = \frac{c_{exhaust} - c_0}{c_{OZ} - c_0} \quad (5)$$

$$\varepsilon_T = \frac{T_{exhaust} - T_0}{T_{OZ} - T_0} \quad (6)$$

The global results obtained for the experimental test cases are provided in Tab.3. The average, minimum and maximum values of the operative temperature, PMV and carbon dioxide concentration are provided, as well as the contaminant removal effectiveness and temperature efficiency.

| MIN\|AVG\|MAX | Top (°C) | | | PMV | | | DR (%) | | | C(ppm) | | | $\varepsilon_C$ | $\varepsilon_T$ |
|---|---|---|---|---|---|---|---|---|---|---|---|---|---|---|
| **Case 0** | 24.0 | 25.0 | 25.6 | -0.12 | 0.20 | 0.40 | 0.0 | 0.2 | 2.8 | - | - | - | - | 0.91 |
| **Case 1** | 24.9 | 25.4 | 25.8 | 0.08 | 0.26 | 0.41 | 0.0 | 0.5 | 6.7 | 639 | 680 | 719 | 0.98 | 1.00 |
| **Case 2** | 24.8 | 25.3 | 25.7 | -0.03 | 0.18 | 0.32 | 0.0 | 0.7 | 5.1 | 953 | 1001 | 1069 | 1.00 | 0.97 |

Table 3. Comfort values and ventilation efficiency obtained from the measurements for the tested cases

Overall, an excellent indoor environment quality is obtained for the studied supplied air conditions. A satisfactory operative temperature is obtained, as well as PMV value under 0.5. Furtermore, the draught risk is limited for all cases, not exceeding a maximum value of 6.7% of dissatisfied. The $CO_2$ concentration reaches an acceptable mean value of 1001ppm for Case 2, where two occupants are in the room. The contaminant removal effectiveness is close to 1, which means that the mixing strategy is efficient, and that the heat and $CO_2$ generated by the occupants are efficiently disposed of. The contaminant removal strategy is illustrated on Fig. 4, where the streamlines from the $CO_2$ injection colored in $CO_2$ concentration are displayed. The injected $CO_2$ is immediately entrained into the buoyant plume and brought to the upper part of the room, and is then entrained into the air jet where it is cooled down and falls in the occupied zone with a lower $CO_2$ concentration. In this case, the polluant sources are associated with the heat sources, the ventilation strategy is hence efficient. However, many indoor air pollutants (VOC, aerosols…) are emitted from passive sources. It would be interesting to determine wether the studied system would be as efficient to remove such kind of polluants.

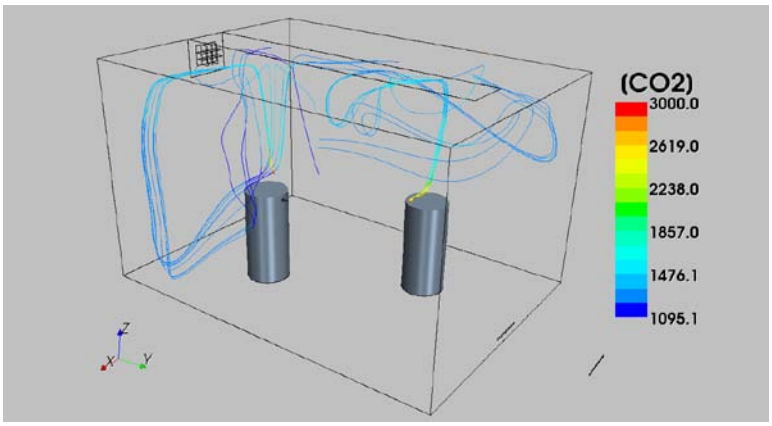


Figure 4. Streamlines colored in CO2 concentration for Case 2

**Influence of the heat sources on the airflow pattern**

The analysis of the global temperature and velocity values gives valuable information on the influence of the heat sources on the airflow in the room and on the resulting comfort. The mean, median, minimum and maximum values of the air temperature and air velocity for the experimental cases are plotted on Fig.5. All test cases are performed at the same air change rate. It appears that the air velocity in the occupied zone is higher with heat sources (Case 1 and Case 2), due to the entrainment of the ambient air into the buoyant plumes. It also stresses that an increase of the air velocity causes the distribution of the air temperature to be more homogeneous in the occupied zone, which is consistent with a mixing ventilation strategy.

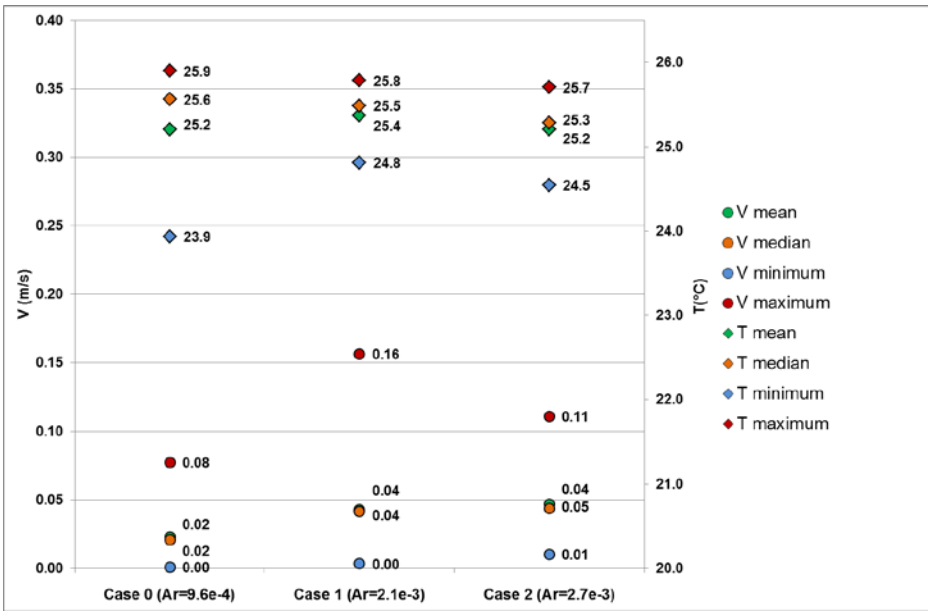


Figure 5. Mean, median, minimum and maximum values of the air temperature and air velocity for the experimental cases

However, the maximum velocity is higher for Case 1 than for Case 2, which indicates that the airflow maybe not be the same for both cases. The velocity streamlines colored in temperature and velocity vectors in the middle plane obtained from the CFD simulations for all three cases are presented in Fig.6 and provide interesting information about the airflow patterns in the room.

In Case 0, the jet is attached to the ceiling thanks to the Coandă effect and goes straight forward, thus reaching the opposite wall. In Case 1 and Case 2, the airflow is tridimensional and follows a clockwise path in the test room. This results from the non-symmetric placement of the dummies. The air jet issued from the diffuser is first deflected to the left by the buoyant plume of the dummy 1. The influence of the heat sources on the airflow is emphasized by the presence of recirculation bubbles above the dummies. The jet then separates from the ceiling and drops slightly in the occupied zone before hitting the opposite wall. It is then deflected backwards toward the occupied zone where it is again entrained in the buoyant plumes and in the air jet. The location and power of the internal gains thus greatly influence the air flow pattern in the room.
Furthermore, it can be seen on the velocity vectors that the jet remains attached to the ceiling longer in Case 0 and Case 1 than in Case 2, which highlights the influence of the supplying conditions on the airflow. However, this influence is hard to pinpoint because of the varying occupancy in the different cases. Hence, a parametric study is performed on the supplying conditions where occupancy is kept constant.

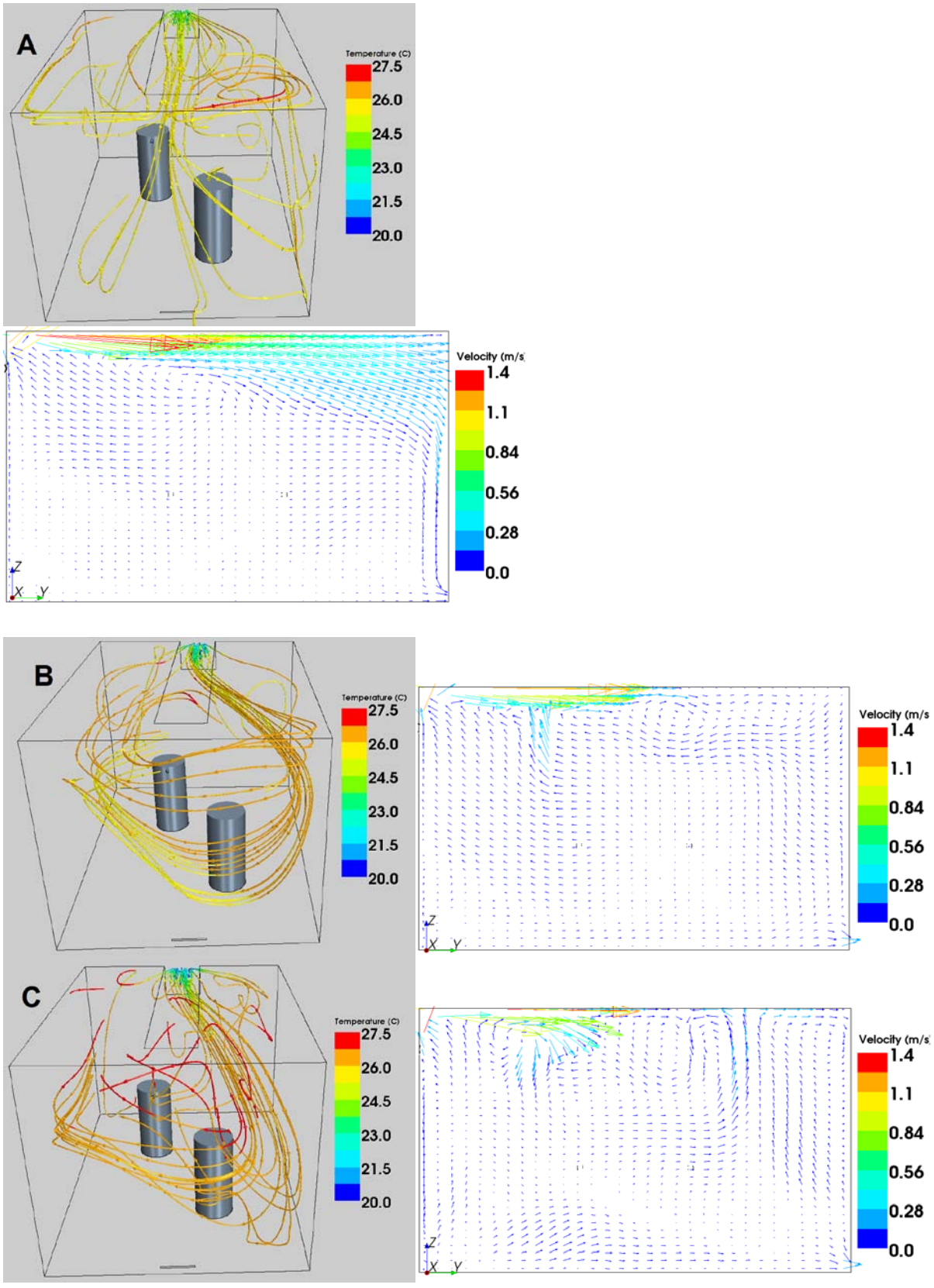


Figure 6. 3D velocity streamlines colored in temperature and velocity vectors in the middle plane. a) Case 0, b) Case 1, c) Case 2.

## Parametric study on the supplying conditions

The choice of the inlet air flow rate and air temperature is crucial during the room air distribution system design, in order to reach the desired IEQ level. Therefore, additional simulations are performed for cases that were not tested experimentally, in order to evaluate the influence of the supplying conditions on the airflow pattern and on the resulting IEQ. The cooling power brought by the supply, the internal gains, the wall temperatures and the $CO_2$ source are kept constant (corresponding to Case 1), while different inlet air flow rates and supply temperatures are considered. The conditions of the tested cases are listed in Tab.4.

| | **Qinlet** | | **Tinlet** | **Toutlet** | **Toz-Tinlet** | **Ar0** | **Re0** |
|---|---|---|---|---|---|---|---|
| | m3/h | ACH | °C | °C | °C | - | - |
| **Case 1** | 57.0 | 1.66 | 17.0 | 25.3 | 8.3 | 2.1E-03 | 17247 |
| **Case $1^-$** | 34.3 | 1.00 | 11.7 | 25.3 | 14.1 | 1.0E-02 | 10722 |
| **Case $1^+$** | 85.7 | 2.50 | 19.7 | 25.8 | 6.2 | 6.8E-04 | 25497 |

Table 4. Supplying conditions for the parametric study

The air flow rate should be high enough to maintain an acceptable air quality, but low enough to not cause any draughts in the occupied zone. A way to define the maximum air flow rate is to choose a maximum velocity allowed in the occupied zone, or at the upper limit of the occupied zone (1,8 m), for instance 0.15 m/s [9]. Buoyant plumes may be responsible for draught as well, but the high air velocity resulting from the dummy is not taken into account in the following maximum air velocity values, the studied parameter being the supplied air conditions.

The contaminant removal effectiveness and temperature efficiency for the three tested cases are displayed in Tab. 5. Compared to Case 1, both Case $1^-$ and Case $1^+$ display a better mixing in the occupied zone, which is translated into a better temperature efficiency.

| | $\varepsilon_C$ | $\varepsilon_T$ | $V_{mean}$ | $V_{max\_1.8m}$ | $V_{max\_OZ}$ |
|---|---|---|---|---|---|
| **Case 1** | 0.98 | 0.94 | 0.04 | 0.14 | 0.14 |
| **Case $1^-$** | = | + 0.02 | + 0.01 | + 0.13 | + 0.13 |
| **Case $1^+$** | + 0.05 | + 0.02 | + 0.04 | - 0.01 | + 0.06 |

Table 5. Contaminant removal effectiveness, temperature efficiency, mean, maximum and maximum velocity et Z = 1.8m in the OZ, compared to Case 1.

However, a different phenomenon is responsible for the increased mixing in both cases. In Case $1^-$, the cold air jet seperates from the ceiling because of the high Archimedes number and drops into the occupied zone, as shown on Fig.7a. Consequently, the mixing is increased, but so is the draught risk with a maximum air velocity of 0.27 m/s in the occupied zone. In Case $1^+$, the jet reaches the opposite wall thanks to the higher air flow rate. The latter also explains the increased mixing, caused by an higher entrainment of the ambiant air into the cold air jet. But this is then responsible for a maximum air velocity at the ankle level of the occupied zone of 0.20 m/s, which results from the jet hitting the opposing wall and being deflected backwards. Therefore, it appears that a low enough Archimedes number which would ensure that the jet would not fall into the occupied zone is not a sufficient condition to guarantee that a high draught risk may not occur, caused by locally high values of air velocity.

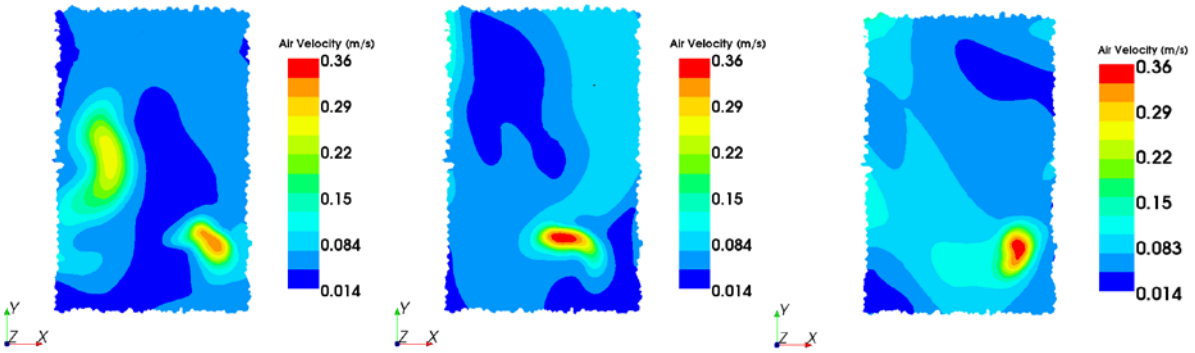


Figure 7. Velocity contours at the upper limite of the occupied zone : Z = 1,8 m. a) Case $1^{-}$ , Ar0 = 1.0E-2 b) Case 1, Ar0 = 2.1E-3 c) Case $1^{+}$, Ar = 6.8E-4

## CONCLUSION

The summer thermal comfort and the ventilation efficiency have been assessed in a test room using a wall-mounted mixing diffuser. Both experimental measurement and CFD simulations have been used. An excellent indoor environment quality has been obtained in the tested conditions. It has been found that the location of the heat sources in respect to the location of the air diffuser plays a major role on the airflow in the room and on the resulting IEQ. This emphasises that the location and power of the heat sources should be taken into account during the design of an air distribution system. Furthermore, it appeared that predicting the throw of the cold air jet to ensure that it does not fall in the occupied zone, or predicting the average air velocity in the occupied zone with the Archimedes number may not ensure that there would not be locally high values of air velocity responsible for local discomfort by draught. It would therefore be advised to perform new CFD simulations to predict the airflow whenever a new room geometry is considered.

## ACKNOWLEDGEMENTS

This study is part of the HABISOL-VABAT programme and is supported by the French National Agency of Research (ANR), which is gratefully acknowledged.

## REFERENCES

[1] Lan, L., Wargocki, P., Wyon, D.P., and Lian, Z. 2011. *Effects of thermal discomfort in an office on perceived air quality, SBS symptoms, physiological responses, and human performance*, Indoor Air 21, 376–390.

[2] Costa, J.J., Oliveira, L.A., and Blay, D. 1999. *Test of several versions for the k-e type turbulence modeling of internal mixed convection flows*, Int. Journal of Heat and Mass Transfer 42, 4391-4409.

[3] Fontaine, J.R., Rapp, P., Koskela, H., and Niemelä, R. 2005. *Evaluation of air diffuser flow modeling methods experiments and computational fluid dynamics simulations*, Building and Environment 40, 377-389.

[4] Cehlin, M., and Moshfegh, B. 2010. *Numerical modeling of a complex diffuser in a room with displacement ventilation*, Building and Environment 45, 2240-2252.

[5] EN 15251. 2007. *Indoor environmental input parameters for design and assessment of energy performance of buildings- addressing indoor air quality, thermal environment, lighting and acoustics*, CEN, Brussels.

[6] Fanger, P.O. 1970. *Thermal Comfort*, Copenhagen: Danish Technical Press.

[7] EN 7730. 2005. *Analytical determination and interpretation of thermal comfort using calculation of the PMV and PPD indices and local thermal comfort criteria.*
[8] Sandberg, M. 1981. *What is Ventilation Efficiency?*, Building and Environment 16, No. 2, 123-135.
[9] Nielsen, P.V. 2007. *Analysis and design of room air distribution systems*, HVAC&R Research 13, 987-997.